The circadian gene Arntl2 on distal mouse chromosome 6 controls thymocyte apoptosis

Basile Lebailly, Francina Langa, Christian Boitard, Philip Avner, Ute Christine Rogner

The circadian gene Arntl2 *on distal mouse chromosome 6 controls thymocyte apoptosis*

Basile Lebailly, Francina Langa, Christian Boitard, Philip Avner & Ute Christine Rogner

Mammalian Genome

ISSN 0938-8990

Mamm Genome
DOI 10.1007/s00335-016-9665-4

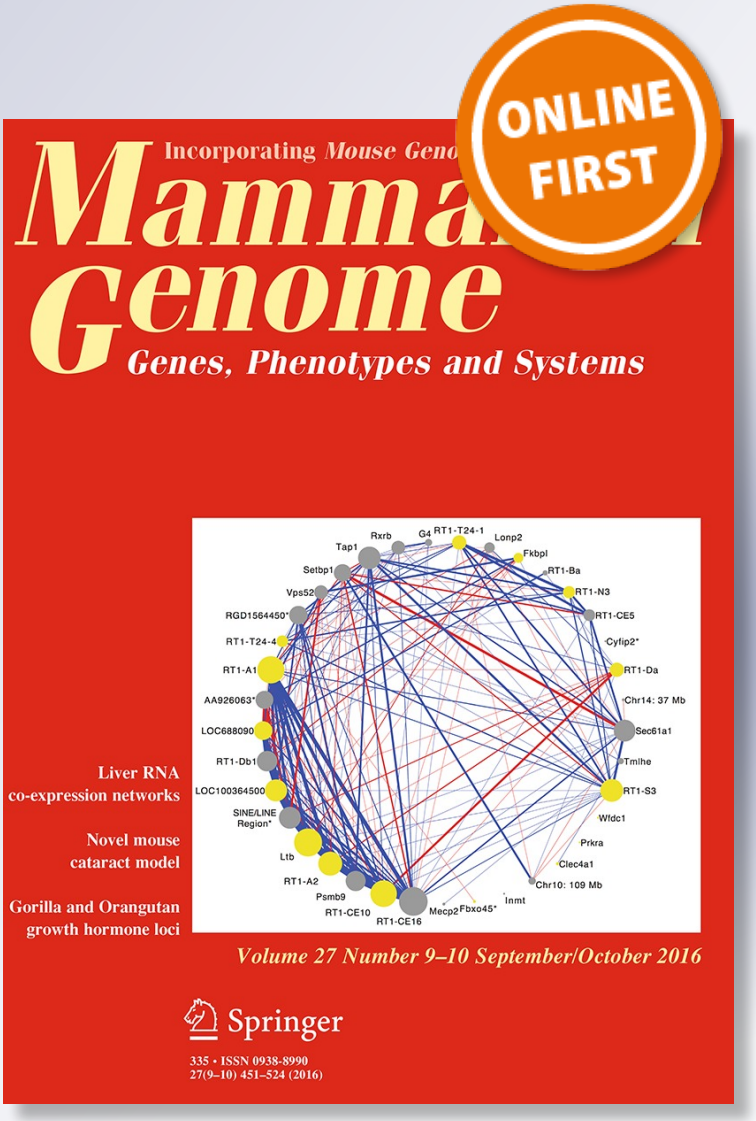

Springer

Mamm Genome
DOI 10.1007/s00335-016-9665-4

The circadian gene *Arntl2* on distal mouse chromosome 6 controls thymocyte apoptosis

Basile Lebailly[1,2] · Francina Langa[3] · Christian Boitard[4] · Philip Avner[1] · Ute Christine Rogner[1,4]

Received: 25 May 2016 / Accepted: 11 September 2016

Abstract Nonobese diabetic (NOD) mice are a model for type 1 diabetes that displays defects in central immune tolerance, including impairment of thymocyte apoptosis and proliferation. Thymocyte apoptosis is decreased in NOD/Lt mice compared to nondiabetic C3H/HeJ and C57BL/6 mice. Analysis of a set of NOD.C3H and NOD.B6 congenic mouse strains for distal chromosome 6 localizes the phenotype to the 700 kb *Idd6.3* interval. *Idd6.3* contains the type 1 diabetes candidate gene aryl hydrocarbon receptor nuclear translocator-like 2 (*Arntl2*), encoding a circadian rhythm-related transcription factor. Newly generated *Arntl2*$^{-/-}$ mouse strains reveal that inactivation of the B6 allele of *Arntl2* is sufficient to both decrease thymocyte apoptosis and proliferation. When expressed from C3H or B6 alleles, ARNTL2 inhibits the transcription of interleukin 21 (*Il21*), a major player in the regulation of immune responses. IL-21 injection abolishes the B6 allele-mediated decrease of apoptosis and proliferation. Interestingly, IL-21 also leads to an increase in thymic proinflammatory Th17 helper cells. Our results identify *Arntl2* as a gene controlling thymocyte apoptosis and proliferation along with Th17 development through the IL-21 pathway.

Introduction

The *Idd6* locus on distal chromosome 6 is a type 1 diabetes susceptibility locus of the nonobese diabetic (NOD) mouse (Smink et al. 2005) that protects against spontaneous diabetes when replaced by alleles from C57BL/6 (B6) or C3H/HeJ (C3H) mice (Bergman et al. 2003; Carnaud et al. 2001; Rogner et al. 2001). B6 alleles at *Idd6* have also been shown to increase thymocyte apoptosis and proliferation (Bergman et al. 2003, 2001; Penha-Goncalves et al. 1995), mechanisms that have been suggested to increase the negative selection of thymocytes against self-antigens.

Genetic dissection using NOD.C3H congenic strains revealed that the *Idd6.3* subinterval is responsible for the control of diabetes in splenocyte transfer assays (Hung et al. 2006). Compared to controls, splenocytes from NOD.C3H congenic mice with C3H alleles at *Idd6.3* transfer diabetes less efficiently, and these congenic mice exhibit lower numbers of interleukin-21 (IL-21)-producing CD4$^+$ T cells in the spleen and thymus (Lebailly et al. 2014). The lower numbers of CD4$^+$IL-21$^+$ T cells correlate strongly with decreased numbers of Th17 and Th2 effector cells. Gene expression studies suggested that the aryl hydrocarbon receptor nuclear translocator-like 2 (*Arntl2*) gene located in *Idd6.3* directly controls *Il21*

Electronic supplementary material The online version of this article (doi:10.1007/s00335-016-9665-4) contains supplementary material, which is available to authorized users.

✉ Ute Christine Rogner
ute.rogner@inserm.fr

1 Mouse Molecular Genetics Laboratory, CNRS URA 2578, Institut Pasteur, 25 rue du Docteur Roux, 75015 Paris, France

2 University Pierre and Marie Curie, Cellule Pasteur UPMC, 25 rue du Docteur Roux, 75015 Paris, France

3 Mouse Genetics Engineering Center, CNRS URA 2578, Institut Pasteur, 28 rue du Docteur Roux, 75015 Paris, France

4 Inserm U1016 - CNRS UMR8104, Groupe Hospitalier Cochin, Université Paris Descartes, 123 boulevard Port-Royal, 75014 Paris, France

Published online: 26 September 2016

expression. The direct targeting of *Il21* by ARNTL2 has been shown by chromatin immunoprecipitation (ChIP) experiments in NOD.C3H congenic mice. These findings led to the hypothesis that the diabetogenic activity of *Idd6.3* splenocytes is controlled by ARNTL2 via the IL-21 pathway. This hypothesis has been reinforced by the fact that ARNTL2 overexpression in $CD4^+$ T cells decreases their diabetogenic activity and decreases IL-21 expression (He et al. 2010b; Lebailly et al. 2014).

IL-21 is a type I cytokine controlling immune responses through interaction with the common γ chain (γc) IL-21 receptor (IL-21R). IL-21 is mostly expressed by Th17 and Th2 subsets of $CD4^+$ T cells and acts on its target genes via activation of the Jak/Stat, MAPK and PI3K pathways (Spolski et al. 2008; Spolski and Leonard 2014; Zeng et al. 2007). IL-21 target cells include T cells, B cells (Ozaki et al. 2004) and natural killer (NK) cells (Frederiksen et al. 2008). High levels of IL-21 boost immune responses and can induce autoimmune reactions (McGuire et al. 2011). In particular, IL-21 promotes T cell survival and thus contributes to T cell homeostasis and expansion (Ostiguy et al. 2007). Moreover, IL-21 not only acts as an activator of effector T cells (Monteleone et al. 2008), but it also antagonizes the suppressive activity of regulatory T cells (Peluso et al. 2007), an effect that is also genetically controlled by *Idd6* (Rogner et al. 2006). Finally, IL-21 controls recovery of thymocytes from apoptosis and is essential for the differentiation of Th17 cells in the thymus via the activation of the RAR-related orphan receptor gamma (RORγ) pathway (Rafei et al. 2013b; Sofi et al. 2010). *Il21* is a candidate gene for T1D and is located in the murine locus *Idd3* (McGuire et al. 2009; Spolski et al. 2008; Sutherland et al. 2009). NOD alleles show increased expression of *Il21* compared to B6 alleles (McGuire et al. 2009).

C3H and B6 alleles of *Arntl2* give rise to proteins that can bind to the RNA polymerase II binding site of the *Il21* promoter, leading to reduced *Il21* transcription. Conversely, NOD *Arntl2* alleles do not translate into proteins that bind to *Il21*, thus leading to high *Il21* expression. In the present work, we show that mutation of the B6 allele of *Arntl2* leads to increased numbers of $CD4^+IL\text{-}21^+$ T cells in spleen and thymus. High levels of *Arntl2* expressed from C3H and B6 alleles in $CD4^+CD8^+$ T cells precede low numbers of IL-21-producing $CD4^+$ T cells. The mutation of *Arntl2* in C57BL/6 and in *Idd6* NOD.B6 congenic mice also decreases the number of apoptotic thymocytes. Exogenous IL-21 decreases apoptosis and increases the number of IL-21-producing $CD4^+$ T cells in the nonmutant N.B6 congenic strain, thus mimicking both $Arntl2^{-/-}$ phenotypes. Our results suggest that *Arntl2* is involved in controlling thymocyte apoptosis and proliferation, which appear to be directly linked to the IL-21 pathway.

Materials and methods

Construction of mouse strains

NOD.C3H congenic mice for *Idd6* have been described previously (Hung et al. 2006; Rogner et al. 2001) (Online Resource 1). The *Arntl2* mutant strain carries the allele $Arntl2^{tm1a(KOMP)Wtsi}$ and has been imported from the UCDavis KOMP Repository (Davis, CA). The C57BL/6-derived *Idd6* interval (including B6 alleles at D6*Mit*14 to D6*Mit*304) has been transferred to the NOD background by crossing females to the NOD/Lt strain, followed by 7 backcrosses and subsequent intercrossing to obtain homozygous mice. In parallel, *Idd6* NOD.B6 congenic mice (including B6 alleles at D6*Mit*14 to D6*Mit*304) were generated as controls (Online Resource 1). Closer examination of the SNPs in the region indicated that the B6-derived interval of both strains includes the marker rs39946360 (144.6 Mb) and excludes the marker rs37447988 (144.4 Mb).

To select for NOD alleles at *Idds* outside of *Idd6*, the following markers were used:

Idd	Markers
Idd5	D1*Mit*18 and D1*Mit*180
Idd13	D2*Mit*395, D2*Mit*17 and D2*Mit*525
Idd3	D3*Nds*6 and D3*Mit*95
Idd10/17/18	D3*Mit*95, D3*Mit*100, and D3*Mit*345
Idd9	D4*Mit*203
Idd11/25	D4*Mit*203 and D4*Mit*59
Idd15	D5*Mit*346 and D5*Mit*48
Idd20/19/	D6*Mit*69, D6*Mit*55
Idd7	D7*Mit*20 and D7*Mit*328
Idd2	D9*Mit*25
Unnamed	D10*Mit*87
Idd4	D11*Mit*339 and D11*Mit*298
Idd14	D13*Mit*16 and D13*Mit*61
Idd8	D14*Mit*110
Idd12	D14*Mit*222
Idd1/16	D17*Mit*34
Idd21	D18*Mit*171, D18*Mit*202, D18*Mit*208, D18*Mit*4

Mutations in the coding region of exon 4 of the NOD-derived *Arntl2* gene were created using the TALEN approach. The constructs pTAL.CMV-T7.012672 and pTAL.CMV-T7.013000, designed to target the sequences TCCAGGTCAGAATTCAT and GGAAAGTCTTCCCCAGA, respectively, were provided and validated by Single Strand Annealing assay (Cellectis, Paris, France). In vitro-transcribed RNA (6–10 ng; Ambion mMESSAGE mMACHINE Kit, Life Technologies, St. Aubin, France)

was pronuclear injected into one-cell stage NOD embryos at the Institut Pasteur Transgenesis Facility (Paris, France). Out of 39 offsprings, two mutants were identified (5 %). NT28 was a female carrying a 25-bp deletion that removes the amino acids (AA) 13–22 and introduces a 2-bp frameshift. NT58 was a male carrying a deletion of AA22 and a conversion of the aspartic acid at AA23 to alanine, but leaving the rest of the gene unaffected. These heterozygous offsprings were crossed to NOD mice and rendered homozygous by intercrossing at the F2 generation.

The absence of protein in the knockout strains was validated by Western blotting using anti-ARNTL2 antibodies (ab86530; Abcam, Paris, France). Diabetes incidence monitoring and diabetes transfer assays were performed as previously described (Lebailly et al. 2014; Rogner et al. 2006). All mice were kept at the Institut Pasteur mouse facility. All animal studies have been approved by the relevant institutional review boards (Comité d'Ethique en Expérimentation Animale CEEA 59, IDF, Paris and C2EA 89, Paris) under protocol numbers 2009-0015 and 2013-125, and the French ministry of higher education and research (Ministère de l'enseignement supérieur et de la recherche) under the reference number 02120.02.

Flow cytometry analysis

Expression of T cell-specific proteins was analysed on a Cyan flow cytometer (Beckman Coulter, Villepinte, France) or a Fortessa flow cytometer (BD Biosciences, Le Pont de Claix, France) after surface and/or intracellular staining using anti-mouse antibodies specific for CD4 (Alexa Fluor 488 or Pacific Blue, BD Biosciences), TCR (PerCP-Cy5.5, BD Biosciences), CD8 (PE-Cy7, BD Biosciences or AF700, eBioscience, Paris, France), IL-17 (Alexa Fluor 488, eBioscience), IL-21 (PE, eBioscience), IFN-γ (Alexa Fluor 700, BD Biosciences), IL-4 (APC, BD Biosciences) and FOXP3 (PerCP-Cy5.5, eBioscience). Briefly, cells were stimulated for 4 h with phorbol myristate acetate (PMA, 25 ng/ml, Sigma, St. Louis, MO) and ionomycin (10 μg/ml, Sigma) in the presence of Brefeldin A (10 μg/ml, BD Biosciences). The cells were then washed in phosphate-buffered saline (PBS) with 0.5 % bovine serum albumin, incubated with eBioscience fixation/permeabilization buffers according to the manufacturer's protocol, and stained with fluorescent antibodies. Analysis of $CD4^+$ thymocyte maturation was performed using anti-mouse antibodies specific for CD4 (eVolve 605, eBioscience), TCR (APC-eFluor 780, eBioscience), CD8 (eVolve 655, eBioscience), CD69 (PE-Cyanine 7, eBioscience), CD5 (APC, eBioscience) and Qa2 (FITC, eBioscience).

Proportions of apoptotic cells in thymic cell populations of 2- to 3-week-old female mice were analysed by flow cytometry using the FITC Annexin V apoptosis detection kit 1 (BD Biosciences). The proportions of apoptotic cells positive for Annexin V, negative for propidium iodide, were calculated amongst the different T cell populations selected on their CD4 and CD8 surface expressions. Phases of the cell cycle were identified using propidium iodide (BD Biosciences) and Ki-67 (eFluor 450, eBioscience) stainings.

All analyses were performed with the FlowJo software package, and statistical analyses employed the Mann–Whitney test. Examples of the gating strategies are shown in the Online Resource 2.

IL-21 injection

Mice were injected daily intraperitoneally with 12.5 μg per kg weight of rIL-21 (594-ML-010, R&D Systems, Minneapolis, USA) diluted in 100 μl of PBS or 100 μl of PBS alone for controls, for 3 days before the testing.

RNA extraction, reverse transcription (RT) and quantitative PCR

Thymic $CD4^+$, $CD8^+$ and $CD4^+CD8^+$ T cells (2×10^5 each) were isolated by labelling with anti-mouse CD4 (Pacific Blue, BD Biosciences) and CD8 antibodies (PE-Cy7, BD Biosciences), followed by cell sorting using a BD FACSAria III. RNA extraction and RT-PCR were done as previously described (Lebailly et al. 2014). All quantifications were performed by real-time PCR in the presence of SYBR Green (Roche, Boulogne–Billancourt, France) on three replicates. The amplification quantification in arbitrary units was performed by the DeltaCt method using three replicates and *Arpo* expression as an endogenous control to normalize mRNA levels. Data were analysed as mean ± SD for single experiments and as mean ± SE for multiple experiments. When appropriate, the differences between two groups were analysed using the Mann–Whitney method.

Chromatin immunoprecipitation (ChIP) was done using the primer pairs Am1–Am4 as previously described (Lebailly et al. 2014). Quantifications were performed by real-time PCR in the presence of SYBR Green (Roche) on three replicates using 50 ng DNA. The results were calculated and normalized as (C_t of IP/C_t of input)/(C_t of control − IP/C_t of input) and compared to binding at the transcription start of *Arpo* (AU = 1) (Lebailly et al. 2014). Data were analysed as mean ± SD for single experiments and as mean ± SE for multiple experiments.

Results

Identification of the *Idd6.3* gene *Arntl2* as candidate for controlling thymocyte apoptosis and proliferation

Previous studies on NOD.B6 congenic strains had shown that the locus *Idd6* is involved in the control of thymocyte apoptosis and proliferation (Bergman et al. 2003, 2001; Penha-Goncalves et al. 1995). Our results confirm such findings for C57BL/6 mice and show that also C3H/HeJ mice exhibit higher numbers of apoptotic T cells in the thymus compared to NOD/Lt mice. The effect on apoptosis in these strains was found for double-positive (DP) $CD4^+CD8^+$ T cells ($P = 0.001$ for C3H and $P = 0.008$ for B6) and single-positive (SP) $CD4^+$ T cells ($P = 0.001$ for C3H and $P = 0.008$ for B6), and in C3H mice for SP $CD8^+$ T cells ($P = 0.001$) (Fig. 1a–c). Further analysis of our NOD.C3H congenic mice showed that C3H alleles at *Idd6* in strain 6.VIII gave results comparable to C3H mice ($P > 0.2$ against C3H, $P = 0.001$ against NOD for all cell types). Amongst the subcongenic strains, the 6.VIIIa strain (C3H alleles at *Idd6.1*) showed apoptosis comparable to NOD ($P > 0.18$ for all cell types), whilst strains 6.VIIIb (*Idd6.2*) and 6.VIIIc (*Idd6.3*) showed results similar to NOD ($P < 0.02$ for all cell types). These results point to a candidate interval of 623-kb controlling thymocyte apoptosis (D6*Mit*373 to D6*Mit*15, Mouse Ensembl Release 84), overlapping the previously described 3-Mb interval controlling resistance to apoptosis distal to D6*Mit*200 on mouse chromosome 6 (Bergman et al. 2003).

We therefore addressed the question if the *Idd6.3* candidate gene *Arntl2* is involved in thymocyte apoptosis. Like the *Idd6* NOD.C3H strain 6.VIII, the N.B6 strain shows increased apoptosis in all cell types when compared to NOD ($P = 0.001$ for DP and SP $CD4^+$ T cells, $P = 0.011$ for $CD8^+$ cells). Mutation of *Arntl2* in NOD.B6 congenic mice (strain N.B6A2$^-$) decreased apoptosis compared to the N.B6 control congenic strain and gave results similar to NOD mice ($P > 0.142$ for all cell types). In contrast to what was observed in the NOD.C3H congenic strains 6.VIIIa and 6.VIIIc ($P = 0.008$ for all cell types), the effect between the two N.B6 congenics was found in $CD4^+CD8^+$ T cells ($P = 0.008$) and in SP $CD4^+$ T ($P = 0.037$) cells but not significantly in SP $CD8^+$ T ($P = 0.296$) cells. Similar observations were made for C57BL/6 *Arntl2* knockout mice ($P = 0.012$ for DP and SP $CD4^+$, $P = 0.196$ for SP $CD8^+$, B6A2$^-$ compared to B6), suggesting that the apoptosis phenotype is linked to *Arntl2* and independent of the genetic background. The frameshift mutation of *Arntl2* in NOD mice did not have a strong influence on apoptosis ($P = 0.037$ for DP, $P = 0.316$ for SP T cells, NT28 compared to NOD). These results indicate that *Arntl2* is involved in the control of thymocyte apoptosis and suggest that C3H alleles and B6 alleles at *Idd6.3*/*Arntl2* increase thymocyte apoptosis compared to NOD alleles.

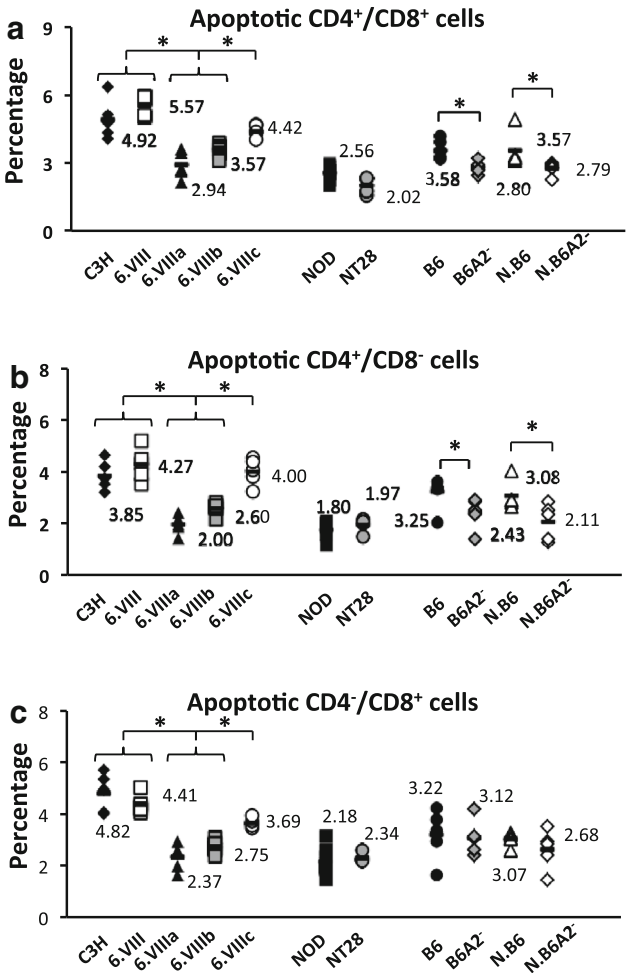

Fig. 1 Proportions of apoptotic cells, positive for Annexin V, negative for propidium iodide, amongst **a** $CD4^+/CD8^+$, **b** $CD4^+/CD8^-$ and **c** $CD4^-/CD8^+$ T cells in the thymus of the different strains of mice (see Online Resource 1) in 3-week-old females. $n = 5$, 6.VIII and 6.VIIIb: $n = 4$, * $P < 0.05$; NOD alleles at *Idd6.3* (strains 6.VIIIa or 6.VIIIb vs C3H, 6.VIII or 6.VIIIc) and *Arntl2* mutation (B6A2$^-$ vs B6, N.B6A2$^-$ vs N.B6) lead to decrease of apoptosis

Higher proportions of apoptotic cells could be indicative of a general loss of thymocytes. However, the total numbers of thymocytes were found to be similar. For example, we found $0.82 \times 10^7 \pm 2.4 \times 10^5$ cells for 6.VIIIa, $0.78 \times 10^7 \pm 12 \times 10^5$ for 6.VIIIc, $0.67 \times 10^7 \pm 15 \times 10^5$ for N.B6A2$^-$ and $0.73 \times 10^7 \pm 2.8 \times 10^5$ for N.B6 ($n = 5$ using 3-week-old females). The proportions of DN, DP and SP cells were also found to be similar. Closer examination of the cell cycle using the N.B6 congenic strains revealed that mutation of *Arntl2* led to significant

changes of the proportions of cells in G0/G1 phase (Fig. 8). Interestingly, the *Arntl2* knockout strain N.B6A2^{-} exhibited higher numbers of cells in G0 phase and lower numbers of cells in G1 phase, indicating that the mutation may lead to cell cycle arrest. However, analysis of developmental T cell (DP1–DP3) and CD4^{+} T cell maturation stages (SP1–SP4) revealed no significant changes (Table 1).

Arntl2 in *Idd6.3* is sufficient to control CD4^{+}IL-21^{+} T cell numbers

We previously described that the presence of C3H alleles at the *Idd6.3* locus increases the number of CD4^{+}IL-21^{+} T cells in the spleen and thymus of NOD.C3H congenic mice (Lebailly et al. 2014). Further analysis revealed that C3H/HeJ mice and C57BL/6 mice produce significantly lower percentages of CD4^{+}IL-21^{+} T cells compared to NOD/Lt mice in the spleen and thymus (Figs. 2a, 3a). These differences in CD4^{+}IL-21^{+} T cells are genetically linked to the *Idd6* locus, as shown by the NOD.C3H 6.VIII strain and by the newly generated *Idd6* NOD.B6 congenic strain N.B6. Further analysis of *Idd6* NOD.C3H congenic mice showed that the phenotype is exclusively linked to *Idd6.3* (strain 6.VIIIc), whilst the loci *Idd6.1* (strain 6.VIIIa) and *Idd6.2* (strain 6.VIIIb) are not implicated (Figs. 2a, 3a).

To address the question whether *Arntl2* alone is sufficient to control the number of CD4^{+}IL-21^{+} T cells, we tested our newly created knockout strains. Using N.B6 congenic strains, we found that *Arntl2* mutation leads to an increase in CD4^{+}IL-21^{+} T cells. Again, differences were found in both spleen and thymus. *Arntl2* mutation in C57BL/6 gave similar results, and the frameshift *Arntl2* mutation in the NT28 strain had no effect on the number of CD4^{+}IL-21^{+} T cells compared to NOD mice (Figs. 2a, 3a). These results demonstrate that *Arntl2* is sufficient for controlling the production of CD4^{+}IL-21^{+} T cells. The phenotype is independent of the genetic background. These differences in IL-21-producing cells were found in thymic CD4^{+} T cells; however, we detected no differences in thymic CD4^{+}CD8^{+} and CD8^{+} T cell populations, for which we observed less than 0.1 % IL-21^{+} T cells for all strains.

We further observed that the differences in IL-21-producing CD4^{+} T cells correlated well with differences in CD4^{+}IL-17^{+} T cells (Figs. 2b, 3b), consistent with the notion that amongst CD4^{+} T cells, the Th17 subset is the main source of IL-21. We also examined if the previously described difference in Th2 cell numbers were present in the knockout strains (Lebailly et al. 2014). The number of CD4^{+}IL4^{+} T cells was significantly increased in the thymus of the N.B6A2^{-} strain compared to the N.B6 strain. Interestingly, the findings were not confirmed for the spleen, and the mutations on the B6 and NOD genetic background had no effect. This could indicate that *Arntl2* is not tightly controlling Th2 numbers. The *Arntl2* mutation did neither influence Th1 (CD4^{+}IFN-γ^{+}) cell numbers (Figs. 2d, 3d) nor the numbers of regulatory CD4^{+}FOXP3^{+} T cells (see below).

We also observed that all strains with higher percentages of IL-21-producing CD4^{+} T cells exhibited less apoptotic cells in the thymus, indicating that these two phenotypes are genetically linked. This suggested that high levels of IL-21 may reduce thymocyte apoptosis and that *Arntl2* may control this pathway.

Table 1 Numbers and percentages of immune cells per one million thymocytes of 3-week old female mice

Cell type (marker)	Strain N.B6 ($n = 5$)	Strain N.B6A2^{-} ($n = 5$)
CD4^{-}CD8^{-}	59437 (5.99 %) ± 9963 (0.99 %)	63,437 (6.36 %) ± 9245 (0.92 %)
CD4^{+}CD8^{+} (total)	777,366 (77.79 %) ± 55,274 (5.53 %)	753,772 (75 %) ± 62,392 (6.31 %)
CD4^{+}CD8^{+} DP1 (TCR^{low} CD5^{low})	587,377 (75.56 % of CD4^{+}CD8^{+}) ± 27,363 (3.52 %)	597,891 (79.32 % of CD4^{+}CD8^{+}) ± 972,365 (1.29 %)
CD4^{+}CD8^{+} DP2 (TCR^{int} CD5^{hi})	83,255 (10.71 % of CD4^{+}CD8^{+}) ± 22,388 (2.88 %)	62,939 (8.35 % of CD4^{+}CD8^{+}) ± 9459 (1.255 %)
CD4^{+}CD8^{+} DP3 (TCR^{hi} CD5^{int})	42,599 (5.48 % of the CD4^{+}CD8^{+}) ± 6607 (0.85 %)	33,768 (4.48 % of the CD4^{+}CD8^{+}) ± 3693 (0.49 %)
CD4^{+}CD8^{-} (total)	127,637 (12.76 %) ± 28,155 (2.81 %)	150,960 (15.1 %) ± 38,248 (3.82 %)
CD4^{+}CD8^{-} SP1/2 (CD69^{+} Qa2^{-})	96,340 (75.48 % of CD4^{+}CD8^{-}) ± 19,490 (15.27 %)	112,208 (74.32 % of CD4^{+}CD8^{-}) ± 15,234 (10.09 %)
CD4^{+}CD8^{-} SP3 (CD69^{-} Qa2^{-})	14,691 (11.51 % of CD4^{+}CD8^{-}) ± 2042 (1.6 %)	19,398 (12.85 % of CD4^{+}CD8^{-}) ± 3698 (2.45 %)
CD4 + CD8^{-} SP4 (CD69^{-} Qa2^{+})	14,001 (10.97 % of CD4^{+}CD8^{-}) ± 7530 (5.89 %)	21,949 (14.54 % of the CD4^{+}CD8^{-}) ± 3170 (2.1 %)
CD4^{-}CD8^{+}	35,861 (3.59 %) ± 3999 (0.4 %)	33,130 (3.31 %) ± 4064 (0.41 %)

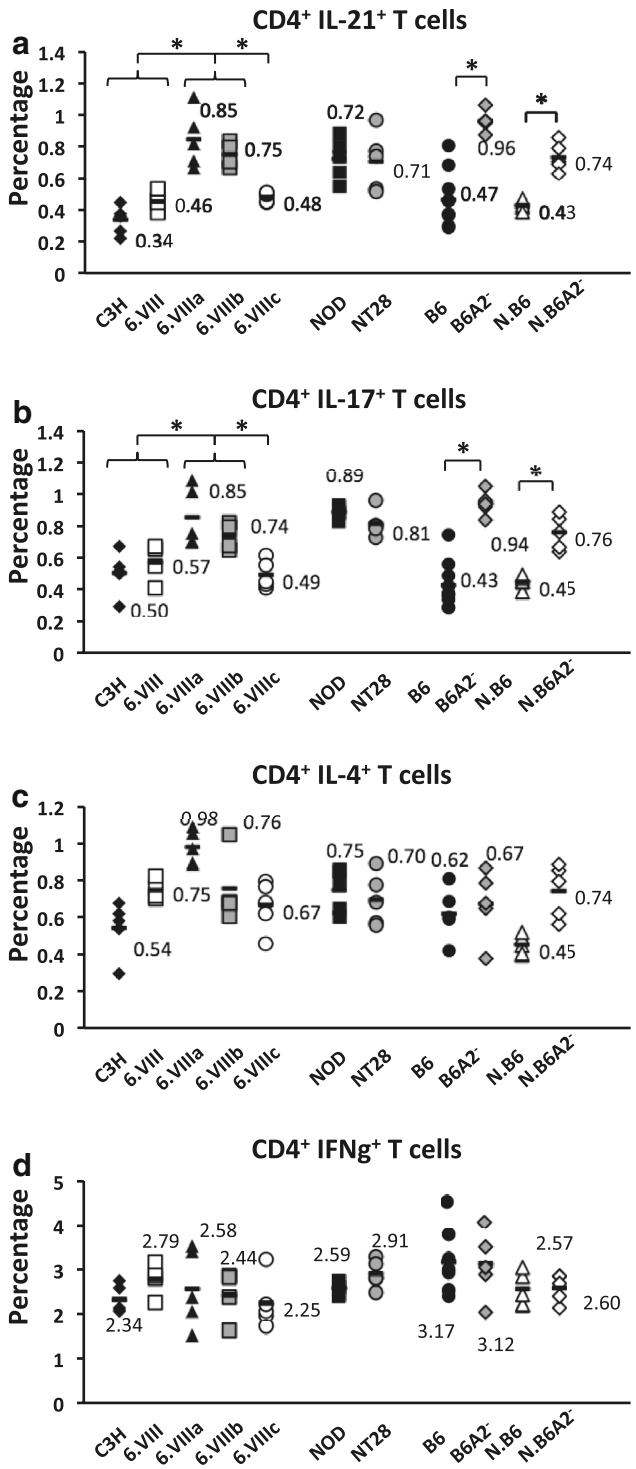

Fig. 2 Proportions of different types of immune cells: **a** $CD4^+IL\text{-}21^+$, **b** $CD4^+IL\text{-}17^+$, **c** $CD4^+IL\text{-}4^+$ and **d** $CD4^+IFN\gamma^+$ in the thymus of 3-week-old females. $n = 5$: 6.VIII and 6.VIIIb, $n = 4$: B6. $n = 10$, * $P < 0.05$

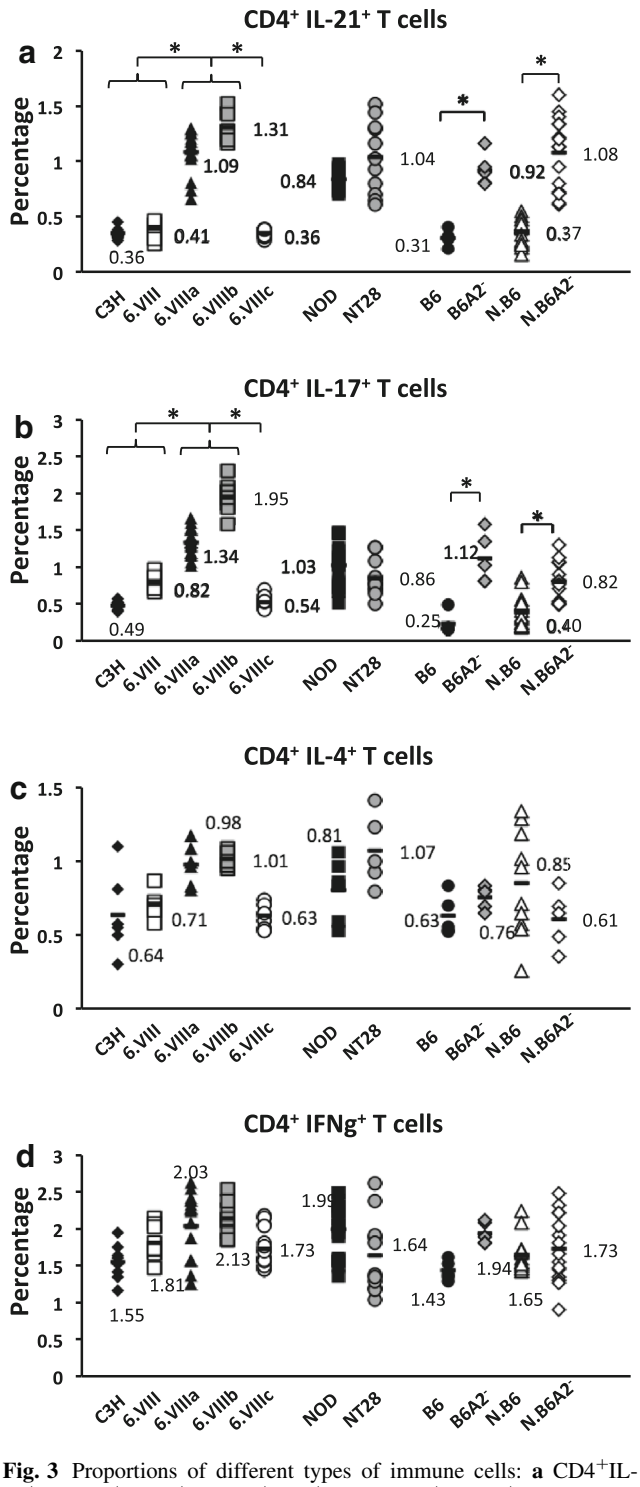

Fig. 3 Proportions of different types of immune cells: **a** $CD4^+IL\text{-}21^+$, **b** $CD4^+IL\text{-}17^+$, **c** $CD4^+IL\text{-}4^+$ and **d** $CD4^+IFN\text{-}\gamma^+$ in the spleen of 5- to 6-week-old females of the different mouse strains. C3H, 6.VIII, 6.VIIIb: $n = 9$; 6.VIIIa, 6.VIIIc, NOD: $n = 19$; NT28: $n = 11$, B6, $B6A2^-$: $n = 5$; N.B6, $N.B6A2^-$: $n = 15$, * $P < 0.05$

ARNTL2 alleles exhibit variations in their coding sequences

Since we have previously shown that C3H alleles of *Arntl2* give rise to proteins that can bind to the promoter of the *Il21* gene, we validated by ChIP that the B6 alleles of *Arntl2* also give rise to proteins that can bind to the RNA polymerase II binding site 922 bp upstream of the first exon (Fig. 4a) in this promoter. Mutation of the B6 allele abolished the binding, and no binding was detected for NOD *Arntl2* alleles compared to C3H (Lebailly et al. 2014) and B6 (Fig. 4b) alleles. As previously reported, we did not detect any binding of the ARNTL2 partners ARNTL1 or CLOCK at this site of interaction (not shown).

The canonical sequence of the ARNTL2 protein comprises 579 amino acids (AA), including four conserved domains (bHLH AA48–101, PAS1 AA119–190, PAS2 AA296–366 and PAC AA371–414). To explore if variations in the ARNTL2 protein sequence may explain the absence of binding of the NOD protein to the *Il21* promoter, we examined the previously published sequences (Hung et al. 2006; Stewart et al. 2003) together with more recent polymorphisms included in the Ensembl database and annotated by the Sanger Mouse Genomes Project. From a total of 62 variants affecting the coding region, we eliminated the synonymous variants and those that were not polymorphic between NOD/Lt, C3H/HeJ and C57BL/6 strains from our further analysis. From the remaining 15 variants, 5 were different between NOD and C3H, 13 between NOD and B6, and 12 between C3H and B6. Interestingly, the NOD allele differs in only 3 coding variants from both C3H and B6 alleles at AA71, 450 and 481 (Table 2). The variant at AA71 is located in the bHLH DNA-binding domain and appears to be the only variant with a low SIFT value (Ng and Henikoff 2001; Sim et al. 2012), predicting that the leucine to methionine replacement in the NOD allele might be deleterious for protein function. Such prediction does not exclude that the other variations in the NOD sequence have functional effects, although they all locate outside of the conserved domains. Recent publications have shown that the C-terminal domains of the protein can have important roles in the activation or repression of transcriptional activities (Xu et al. 2015).

We next examined *Arntl2* expression levels at different thymocyte differentiation stages. In the NOD.C3H congenics 6.VIIIa and 6.VIIIc, the highest *Arntl2* expression was found in double-positive (DP) $CD4^+CD8^+$ T cells. This result was confirmed in the $N.B6A2^-$ strain compared to the N.B6 strain (Fig. 5d). This indicates that transcriptional changes of *Arntl2* precede the measurable differences of IL-21 expression in $CD4^+$ T cells. In these experiments, increased levels of *Arntl2* correlated with lower expression of *Il21* in $CD4^+CD8^+$ T cells (Fig. 5b, e). No changes in *Il17* transcripts were detected (Fig. 5c), confirming that the increase of Th17 cells in the mutant does not correlate with increased *Il17* transcript levels (Lebailly et al. 2014).

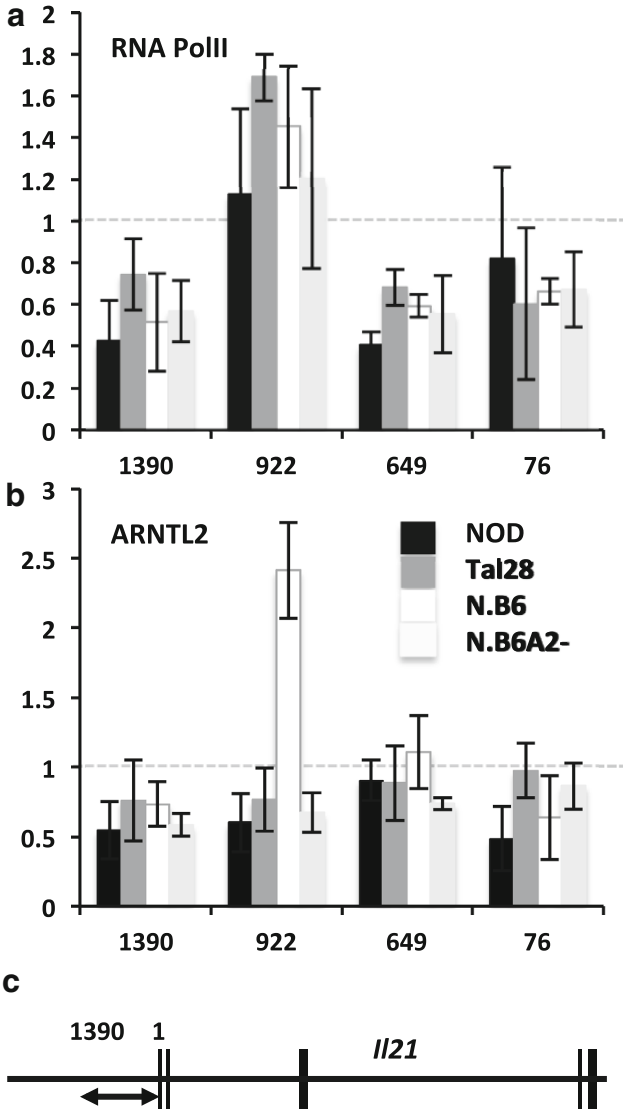

Fig. 4 ChIP analysis of **a** RNA POL II and **b** ARNTL2 on the *Il21* promoter using different mouse strains. Two independent tests (±) SE using splenocytes from three 5-week-old female mice each are shown. The results represent arbitrary units and were calculated and normalized as (C_t of IP/C_t of input)/(C_t of control − IP/C_t of input) and compared to binding at the transcription start of *Arpo* (*dashed grey line*) (Lebailly et al. 2014). Positions are indicated in bps upstream of the coding start of the *Il21* gene at bp 37232618 on mouse chromosome 3 (Ensembl GRCm38.p4). The structure of *Il21* gene (10 kb) is shown in panel (**c**), exons are marked as *black boxes*, the *arrow* marks the promoter region under investigation

Table 2 Codon variants of the ARNTL2 protein

AA residue	Variant identifier	Consequence	Alleles	Resulting codons	Resulting AA	Alleles in			SIFT prediction
						NOD	C3H	B6	
71	rs36388854	Missense	C/A	CTG, ATG	L, M	AA	CC	CC	Deleterious (0)
164	rs48247052	Missense	A/G	ATA, ATG	I, M	GG	GG	AA	Tolerated (0.13)
207	rs29924777	Missense	T/C	TAC, CAC	Y, H	CC	CC	TT	Tolerated (0.9)
213	rs30073811	Missense	A/G	ATG, GTG	M, V	GG	GG	AA	Tolerated (0.31)
423	rs48852525	Missense	T/G	CAT, CAG	H, Q	GG	GG	TT	Tolerated (0.57)
425	rs225458185	Missense	G/A/T	GGC, AGC	G, S	GG	AA	GG	Tolerated (1)
426	rs49229642	Missense	G/A/T	GGC, AGC	G, S	GG	AA	GG	Tolerated (1)
450	rs247782630	Missense	G/A	GTC, ATC	V, I	AA	GG	GG	Tolerated (0.41)
479	rs212813005	Missense	G/A	AGC, AAC	S, N	AA	AA	GG	Tolerated (0.09)
481	rs259733556	Inframe deletion	AGA/−	TCAGAA, TCA	SE, S	(−/−)	(+/+)	(+/+)	No data
494	rs49176210	Missense	A/G	AAT, AGT	N, S	GG	GG	AA	Tolerated (0.76)
494	rs586986482	Missense	AT/GC	AAT, AGC	N, S	GG	GG	AA	Tolerated (0.76)
504	rs49078756	Missense	C/T	CCT, CTT	P, L	TT	TT	CC	Tolerated (0.88)
511	rs50619963	Missense	G/A	GAA, AAA	E, K	AA	AA	GG	Tolerated (0.35)
535	rs50518043	Missense splice variant	G/A	GGT, AGT	G, S	GG	GG	AA	Tolerated (0.52)

Sequence variants leading to amino acid (AA) changes in ARNTL2 in NOD/Lt, C3H/HeJ and C57BL/6 mice. AA 71 locates to the bHLH domain, AA 164 and 207 both to the PAS1 domain

IL-21 administration rescues thymocyte apoptosis and increases Th17 numbers

We next tested if exogenous IL-21 could decrease thymocyte apoptosis (Rafei et al. 2013a). Preliminary tests showed that recombinant IL-21 (rIL-21) doses of 12.5 μg/kg were most effective, whilst higher doses of 25 μg/kg and 50 μg/kg were less effective. Injection of 12.5 μg/kg rIL-21 during 3 days clearly decreased the percentage of apoptotic $CD4^+CD8^+$ and $CD4^+CD8^-$ T cells in the N.B6 congenic strain. The rIL-21 administration reduced apoptosis to similar percentages observed in the $N.B6A2^-$ strain (Fig. 6). IL-21 injection also led to increased numbers of DP and SP cells in G0 phase (Fig. 8) in the N.B6 congenics. No effect of rIL-21 on apoptosis or proliferation was found for the $N.B6A2^-$ knockout mice. Interestingly, also the number of IL-21- and IL-17-producing cells increased in the N.B6 congenic strain after rIL-21 injection, whilst the number of $CD4^+FOXP3^+$ and $CD4^+INF\text{-}\gamma^+$ T cells did not change significantly (Fig. 7). Neither the number of IL-21^+ T cells or of IL-17^+ T cells changed in the knockout mice. This result indicates that the pathways are regulated by IL-21, and that the inhibitory effects of ARNTL2 can be rescued by exogenous IL-21.

Discussion

Genetic control of thymocyte apoptosis in *Idd6*

The NOD mouse displays defects in the selection of T lymphocytes in the thymus. NOD genetic variation influences, for example, the αβ/γδ lineage decision promoted by early expression of transgenic αβ TCRs at the DN stage (Mingueneau et al. 2012). The NOD mouse also displays defects in the mechanism(s) mediating programmed cell death in T lymphocytes (Guler et al. 2005; Leijon et al. 1994). Defects in thymic negative selection are thought to

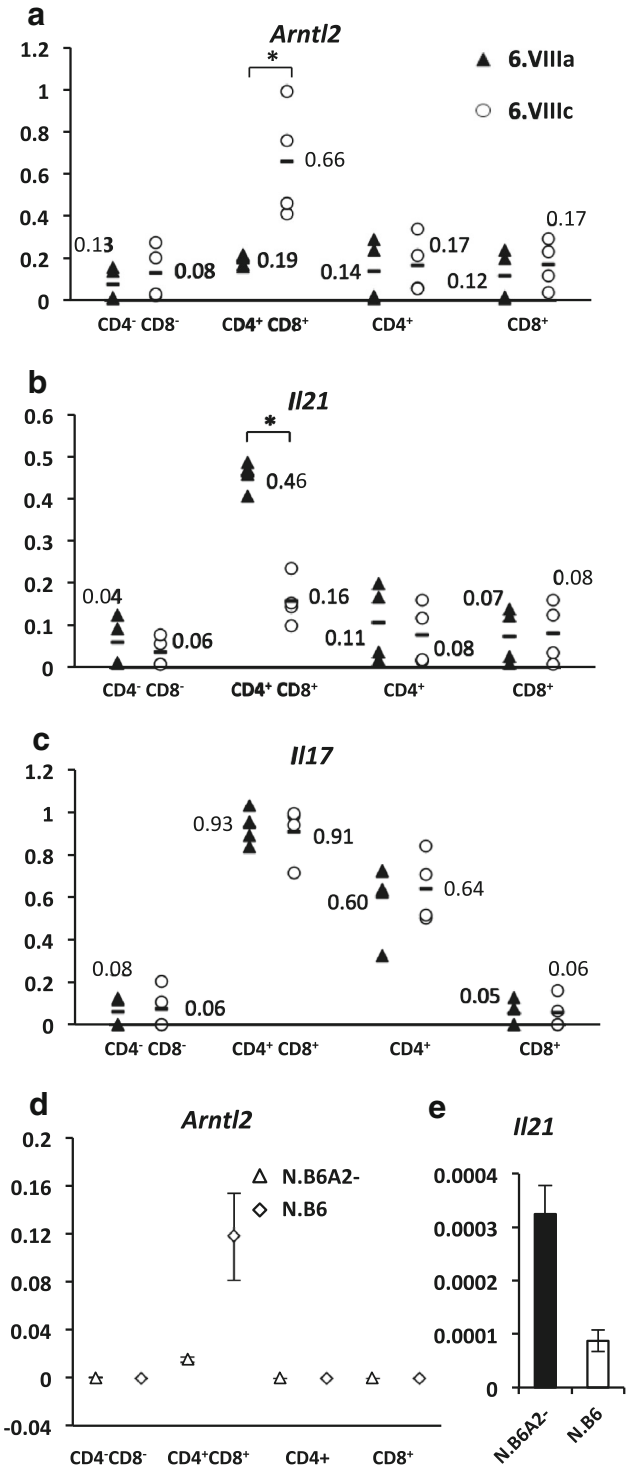

Fig. 5 Expression of **a** *Arntl2*, **b** *Il21* and **c** *Il17* in the different stages of development of the lymphocytes in the thymus of the strains 6.VIIIa and 6.VIIIc. The results are shown as arbitrary units. $n = 4$ using two 2-week-old female mice each. * $P < 0.001$ (Mann–Whitney test). Expression for *Arntl2* in strains N.B6 and N.B6A2^{-} is shown in panel (**d**) (2 experiments ±SE using 2 female mice each). Corresponding expression of *Il21* in CD4^{+}CD8^{+} T cells is shown under (**e**)

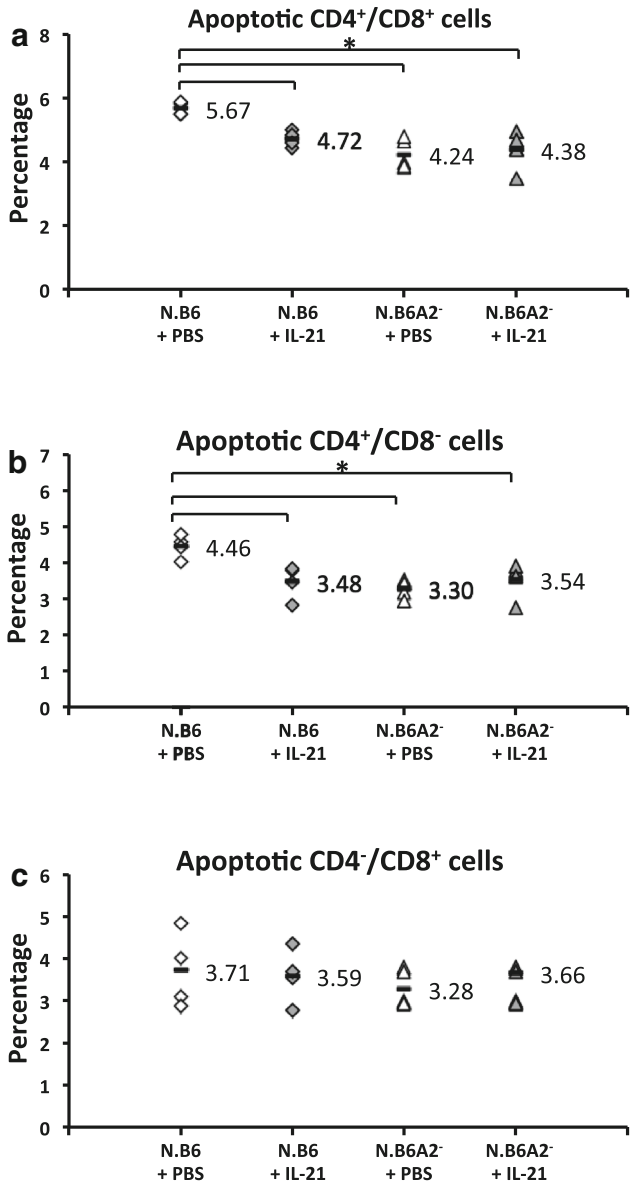

Fig. 6 Proportions of apoptotic cells amongst **a** CD4^{+}/CD8^{+}, **b** CD4^{+}/CD8^{-} and **c** CD4^{-}/CD8^{+} cells in the thymus of 3-week-old females N.B6 or N.B6A2^{-} mice after 3 daily injections with either PBS or IL-21 (12.5 µg/kg). $n = 5$, * $P < 0.05$

result in failure to delete β-cell-reactive T cells, thus contributing to T1D development (Kwon et al. 2005), and autoreactive diabetogenic T cells are likely to result from an inappropriate selection of DP thymocytes in NOD mice.

Previous genetic analyses have mapped T cell proliferative effects and induced apoptosis to *Idd6* and more precisely to the *Idd6.1–Idd6.3* interval (Bergman et al. 2003; 2001, Duarte et al. 2007; Penha-Goncalves et al. 1995). Our present study localizes apoptosis effects in SP and DP T cells to *Idd6* and *Idd6.3*. Both B6 and C3H alleles at *Idd6* increase the number of apoptotic cells compared to NOD alleles. The *Arntl2*$^{-/-}$ NOD.B6 and C57BL/6 mice confirm

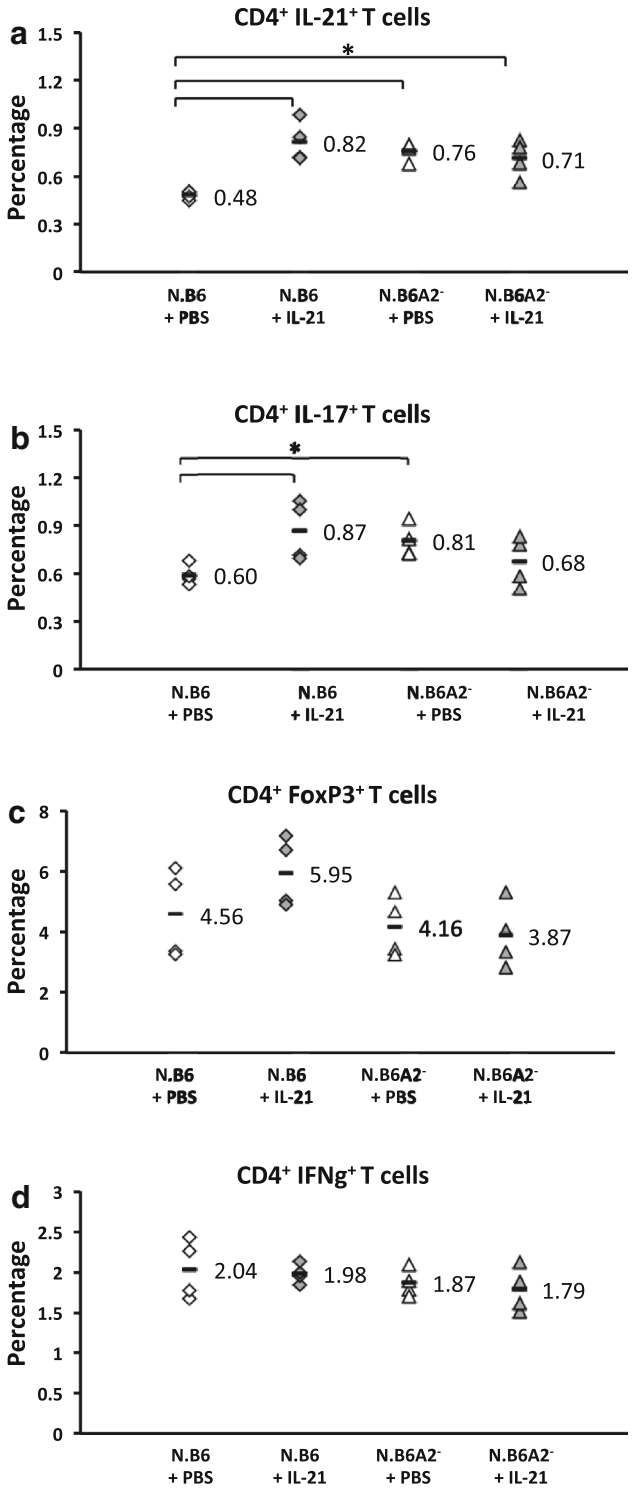

Fig. 7 Proportions of different types of immune cells: **a** $CD4^+IL\text{-}21^+$, **b** $CD4^+IL\text{-}17^+$, **c** $CD4^+FoxP3^+$ and **d** $CD4^+IFN\text{-}\gamma^+$ in the thymus of 3-week-old females N.B6 and N.B6A2$^-$ after three daily injection with either PBS or IL-21 (12.5 µg/kg). $n = 4$. * $P < 0.05$

the result for DP T and SP $CD4^+$ T cells but not for $CD8^+$ T cells. The differences in affected cell populations could be due to the different alleles or due to other genes present in the *Idd6.3* interval. Our results also show that thymocyte apoptosis effects in *Arntl2* knockouts depend on the gene itself but not on the genetic background of the autoimmune NOD model.

Our present results indicate *Arntl2*-related changes in apoptosis and in cell cycle. So far, we could neither detect changes in $CD4^+$ T cell maturation nor in the TCRVβ repertoire (TCRVß chains 2–7, 8.1, 8.2, 9–14, 17) of thymic SP $CD4^+$ and $CD8^+$ T cells. Interestingly, also IL-21 treatment has been shown to not skew the TCRVβ repertoire during recovery from induced thymocyte apoptosis (Rafei et al. 2013a).

Arntl2 and the IL-21 pathway in thymocyte development

We previously suggested and hereby confirm that *Arntl2* controls *Il21* expression (Lebailly et al. 2014). C3H and B6 alleles of *Arntl2* encode proteins that inhibit *Il21* expression; NOD alleles and mutated B6 alleles of *Arntl2* increase the level of *Il21* and the number of IL-21-producing cells in the thymus and spleen.

Our present study shows also that differences in IL-21 expression are related to the differences in *Arntl2* expression in $CD4^+CD8^+$ thymocytes. It has been shown that IL-21 inhibits thymocyte apoptosis (Rafei et al. 2013b) and increases recovery from induced apoptosis (Rafei et al. 2013a). This suggests that the observed changes in IL-21 expression may be related to the differences in apoptosis. Our IL-21 injection studies clearly support this model. IL-21 induces differentiation of Th17 cells (Deenick and Tangye 2007; Sofi et al. 2010; Wei et al. 2007), and higher IL-21 levels could also be responsible for the increased numbers of Th17 cells amongst $CD4^+$ T cells. However, and for both phenotypes, exogenous IL-21 at the applied doses seems inefficient in the *Arntl2*$^{-/-}$ strain. One possible but not exclusive explanation to this may be that the higher endogenous levels of IL-21 have already saturated the pathways.

Arntl2 as a type 1 diabetes candidate gene

Idd6 has been identified as a NOD susceptibility locus in several independent studies. Bergmann et al. (Bergman et al. 2003) already reported protective effects for B6 alleles at *Idd6* in a larger 8 cM interval excluding the NK locus (Carnaud et al. 2001), and Duarte et al. excluded the distal 3 cM interval (D6*Mit*15–D6*Mit*304) from the candidate region (Duarte et al. 2007). Our results suggest that B6 alleles at the D6*Mit*14–D6*Mit*304 interval confer diabetes protection in the NOD mouse (Online Resource 3). Taken together, these data suggested that spontaneous diabetes incidence is decreased when B6 alleles are present

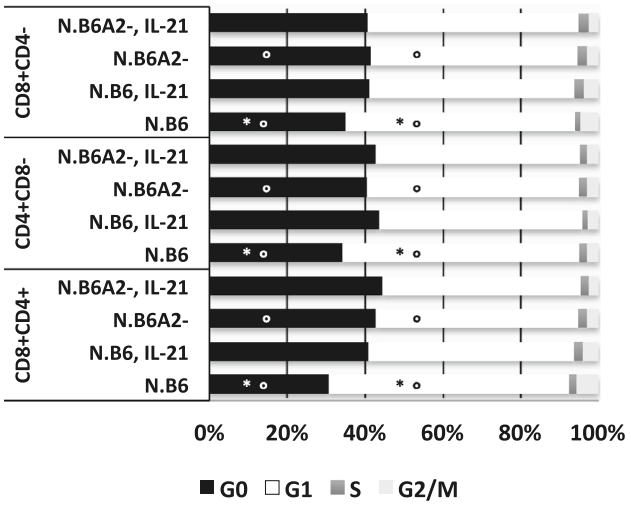

Fig. 8 Cell cycle analysis of thymocytes using propidium iodide and Ki-67 stainings. Percentages of cells in different phases of the cell cycle are shown for five 3-week-old females of strains N.B6 and N.B6A2^{-}, each with or without IL-21 treatment. *Asterisk* $P < 0.05$ for comparison of injection of IL-21 injection versus PBS; *Degree* $P < 0.05$ for comparison between the two strains. The data present one experiment out of two with similar results

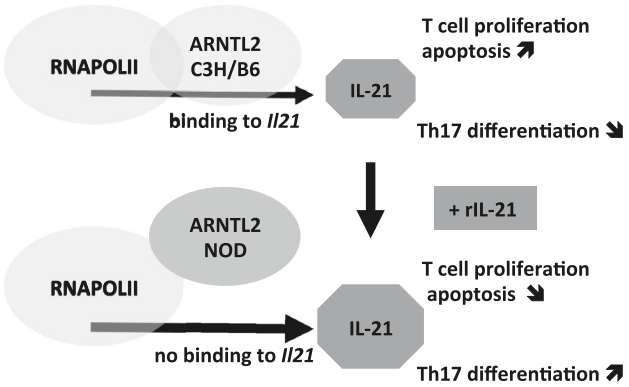

Fig. 9 Model for ARNTL2 action on IL-21 levels in the thymus. ARNTL2 proteins expressed from C3H and B6 alleles bind to *Il21*, resulting in lower numbers of IL21-expressing cells. Low levels of IL-21 lead to increase in apoptosis and T cell proliferation, and decrease of Th17 differentiation, resulting in higher T effector cell ratios. Recombinant IL-21 (rIL-21) can rescue these phenotypes

at the D6*Mit*14–D6*Mit*15 interval, corresponding to the *Idd6.2* locus defined by the NOD.C3H congenics (strain 6.VIIIb) (Hung et al. 2006). The results also suggest that protection in NOD.B6 congenic strains is not controlled by *Idd6.1* and *Idd6.3*. When testing diabetes incidence of the newly created congenic strains, we found that mutation of *Arntl2* alone is clearly not sufficient to alter the spontaneous diabetes incidence in the *Idd6* NOD.B6 congenic strain (Online Resource 3). Also, the mutation of the NOD allele of *Arntl2* (strain NT28) did not significantly affect diabetes incidence compared to NOD control mice generated in the same experiment. At 30 weeks of age, the incidence was 74 % ($n = 23$ females) for control and 57 % ($n = 21$ females) for female mice carrying the frameshift mutation, respectively. Taken together, the data suggest that neither *Idd6.3* nor *Arntl2* alone affects spontaneous diabetes incidence in the congenic strains. One reason may lie in the genetic complexity of the region. It would probably require congenic strains to carry C3H or B6 alleles only at *Idd6.3* to completely clarify this issue. Another reason for the insignificant changes in the knockout may be due to the age-specific action of *Arntl2*-related phenotypes (Lebailly et al. 2014) that are lastly too small to have an impact on the diabetes incidence.

Interestingly and as already observed for the *Idd6.3* locus in the NOD.C3H strains 6.VIIIa and 6.VIIIc, the presence of *Arntl2* strongly decreases diabetes transfer using the NOD.B6 mice as splenocyte donors (Online Resource 3). These results are in line with previous findings that increased *Arntl2* expression in peripheral CD4^{+} T cells induces *Il21* expression and inhibits diabetes development (He et al. 2010a, b), but they require further examination of the cellular and molecular mechanisms involved. Interestingly, the here described altered NOD allele had no effect on diabetes transfer ($n = 5$ for both groups, 80 % diabetic at 12 weeks). It would however require generation of different alleles and expression levels to definitively argue that the NOD *Arntl2* allele has become ineffective in the mouse, at least for its role in the immune system (Fig. 8).

Conclusion

Our work shows that the circadian rhythm-related gene *Arntl2* links control of *Il21* expression to Th17 development and thymocyte apoptosis. In summary, low or absent expression of *Arntl2* leads to increased levels of IL-21, promoting the development of Th17 cells, whilst reducing the ability of other T cells to proliferate, finally reducing the equilibrium between regulatory T cells and proinflammatory T helper cells (Fig. 9).

Acknowledgments We thank Pierre-Henri Commère, Corinne Veron, Chantal Bécourt, Gaelle Chauveau-Le Friec and Abokouo Zago for technical assistance, and Roberto Mallone for correcting the manuscript. The authors acknowledge the financial support of their work by Laboratoire d'Excellence Revive (Investissement d'Avenir; ANR-10-LABX-73), European Foundation for the Study of Diabetes (EFSD)/Juvenile Diabetes Research Foundation (JDRF)/Novo Nordisk Programme, Domaine d'intérêt majeur (DIM): Cardiovasculaire-Obésité-Rein-Diabète (CORDDIM) and by recurrent funding from the Centre national de la recherche scientifique (CNRS), Institut national de la santé et de la recherche médicale (INSERM) and Institut Pasteur.

References

Bergman ML, Penha-Goncalves C, Lejon K, Holmberg D (2001) Low rate of proliferation in immature thymocytes of the non-obese diabetic mouse maps to the *Idd6* diabetes susceptibility region. Diabetologia 44:1054–1061

Bergman ML, Duarte N, Campino S, Lundholm M, Motta V, Lejon K, Penha-Goncalves C, Holmberg D (2003) Diabetes protection and restoration of thymocyte apoptosis in NOD *Idd6* congenic strains. Diabetes 52:1677–1682

Carnaud C, Gombert J, Donnars O, Garchon H, Herbelin A (2001) Protection against diabetes and improved NK/NKT cell performance in NOD.NK1.1 mice congenic at the NK complex. J Immunol 166:2404–2411

Deenick EK, Tangye SG (2007) Autoimmunity: IL-21: a new player in Th17-cell differentiation. Immunol Cell Biol 85:503–505

Duarte N, Lundholm M, Holmberg D (2007) The Idd6.2 diabetes susceptibility region controls defective expression of the Lrmp gene in nonobese diabetic (NOD) mice. Immunogenetics 59:407–416

Frederiksen KS, Lundsgaard D, Freeman JA, Hughes SD, Holm TL, Skrumsager BK, Petri A, Hansen LT, McArthur GA, Davis ID, Skak K (2008) IL-21 induces in vivo immune activation of NK cells and CD8(+) T cells in patients with metastatic melanoma and renal cell carcinoma. Cancer Immunol Immunother 57:1439–1449

Guler ML, Ligons DL, Wang Y, Bianco M, Broman KW, Rose NR (2005) Two autoimmune diabetes loci influencing T cell apoptosis control susceptibility to experimental autoimmune myocarditis. J Immunol 174:2167–2173

He CX, Avner P, Boitard C, Rogner UC (2010a) Downregulation of the circadian rhythm related gene Arntl2 suppresses diabetes protection in Idd6 NOD.C3H congenic mice. Clin Exp Pharmacol Physiol 37:1154–1158

He CX, Prevot N, Boitard C, Avner P, Rogner UC (2010b) Inhibition of type 1 diabetes by upregulation of the circadian rhythm-related aryl hydrocarbon receptor nuclear translocator-like 2. Immunogenetics 62:585–592

Hung MS, Avner P, Rogner UC (2006) Identification of the transcription factor ARNTL2 as a candidate gene for the type 1 diabetes locus Idd6. Hum Mol Genet 15:2732–2742

Kwon H, Jun HS, Yang Y, Mora C, Mariathasan S, Ohashi PS, Flavell RA, Yoon JW (2005) Development of autoreactive diabetogenic T cells in the thymus of NOD mice. J Autoimmun 24:11–23

Lebailly B, He C, Rogner UC (2014) Linking the circadian rhythm gene Arntl2 to interleukin 21 expression in type 1 diabetes. Diabetes 63:2148–2157

Leijon K, Hammarstrom B, Holmberg D (1994) Non-obese diabetic (NOD) mice display enhanced immune responses and prolonged survival of lymphoid cells. Int Immunol 6:339–345

McGuire HM, Vogelzang A, Hill N, Flodstrom-Tullberg M, Sprent J, King C (2009) Loss of parity between IL-2 and IL-21 in the NOD Idd3 locus. Proc Natl Acad Sci USA 106:19438–19443

McGuire HM, Walters S, Vogelzang A, Lee CM, Webster KE, Sprent J, Christ D, Grey S, King C (2011) Interleukin-21 is critically required in autoimmune and allogeneic responses to islet tissue in murine models. Diabetes 60:867–875

Mingueneau M, Jiang W, Feuerer M, Mathis D, Benoist C (2012) Thymic negative selection is functional in NOD mice. J Exp Med 209:623–637

Monteleone G, Pallone F, MacDonald TT (2008) Interleukin-21: a critical regulator of the balance between effector and regulatory T-cell responses. Trends Immunol 29:290–294

Ng PC, Henikoff S (2001) Predicting deleterious amino acid substitutions. Genome Res 11:863–874

Ostiguy V, Allard EL, Marquis M, Leignadier J, Labrecque N (2007) IL-21 promotes T lymphocyte survival by activating the phosphatidylinositol-3 kinase signaling cascade. J Leukoc Biol 82:645–656

Ozaki K, Spolski R, Ettinger R, Kim HP, Wang G, Qi CF, Hwu P, Shaffer DJ, Akilesh S, Roopenian DC, Morse HC 3rd, Lipsky PE, Leonard WJ (2004) Regulation of B cell differentiation and plasma cell generation by IL-21, a novel inducer of Blimp-1 and Bcl-6. J Immunol 173:5361–5371

Peluso I, Fantini MC, Fina D, Caruso R, Boirivant M, MacDonald TT, Pallone F, Monteleone G (2007) IL-21 counteracts the regulatory T cell-mediated suppression of human $CD4^+$ T lymphocytes. J Immunol 178:732–739

Penha-Goncalves C, Leijon K, Persson L, Holmberg D (1995) Type 1 diabetes and the control of dexamethazone-induced apoptosis in mice maps to the same region on chromosome 6. Genomics 28:398–404

Rafei M, Dumont-Lagace M, Rouette A, Perreault C (2013a) Interleukin-21 accelerates thymic recovery from glucocorticoid-induced atrophy. PLoS One 8:e72801

Rafei M, Rouette A, Brochu S, Vanegas JR, Perreault C (2013b) Differential effects of gammac cytokines on postselection differentiation of CD8 thymocytes. Blood 121:107–117

Rogner UC, Boitard C, Morin J, Melanitou E, Avner P (2001) Three loci on mouse chromosome 6 influence onset and final incidence of type I diabetes in NOD.C3H congenic strains. Genomics 74:163–171

Rogner UC, Lepault F, Gagnerault MC, Vallois D, Morin J, Avner P, Boitard C (2006) The Diabetes Type 1 Locus Idd6 Modulates Activity of $CD4^+CD25^+$ Regulatory T-Cells. Diabetes 55:186–192

Sim NL, Kumar P, Hu J, Henikoff S, Schneider G, Ng PC (2012) SIFT web server: predicting effects of amino acid substitutions on proteins. Nucleic Acids Res 40:W452–W457

Smink LJ, Helton EM, Healy BC, Cavnor CC, Lam AC, Flamez D, Burren OS, Wang Y, Dolman GE, Burdick DB, Everett VH, Glusman G, Laneri D, Rowen L, Schuilenburg H, Walker NM, Mychaleckyj J, Wicker LS, Eizirik DL, Todd JA, Goodman N (2005) T1DBase, a community web-based resource for type 1 diabetes research. Nucleic Acids Res 33:D544–D549

Sofi MH, Liu Z, Zhu L, Yu Q, Kaplan MH, Chang CH (2010) Regulation of IL-17 expression by the developmental pathway of CD4 T cells in the thymus. Mol Immunol 47:1262–1268

Spolski R, Leonard WJ (2014) Interleukin-21: a double-edged sword with therapeutic potential. Nat Rev Drug Discov 13:379–395

Spolski R, Kashyap M, Robinson C, Yu Z, Leonard WJ (2008) IL-21 signaling is critical for the development of type I diabetes in the NOD mouse. Proc Natl Acad Sci USA 105:14028–14033

Stewart S, Dykxhoorn DMPD, Mizuno H, Yu EY, An DS, Sabatini DM, Chen IS, Hahn WC, Sharp PA, Weinberg RA, Novina CD (2003) Lentivirus-delivered stable gene silencing by RNAi in primary cells. RNA 9:493–501

Sutherland AP, Van Belle T, Wurster AL, Suto A, Michaud M, Zhang D, Grusby MJ, von Herrath M (2009) Interleukin-21 is required for the development of type 1 diabetes in NOD mice. Diabetes 58:1144–1155

Wei L, Laurence A, Elias KM, O'Shea JJ (2007) IL-21 is produced by Th17 cells and drives IL-17 production in a STAT3-dependent manner. J Biol Chem 282:34605–34610

Xu H, Gustafson CL, Sammons PJ, Khan SK, Parsley NC, Ramanathan C, Lee HW, Liu AC, Partch CL (2015) Cryptochrome 1 regulates the circadian clock through dynamic interactions with the BMAL1 C terminus. Nat Struct Mol Biol 22:476–484

Zeng R, Spolski R, Casas E, Zhu W, Levy DE, Leonard WJ (2007) The molecular basis of IL-21-mediated proliferation. Blood 109:4135–4142